Sustainable Marine Structures
https://journals.nasspublishing.com/sms

ARTICLE

Finite Element Modelling of Hydrogen Embrittlement by Considering Hydrogen Coverage Boundary Conditions

Dario Gravina [1,2], Selda Oterkus [1*], Erkan Oterkus [1]

[1] *Department of Naval Architecture, Ocean and Marine Engineering, University of Strathclyde, G4 0LZ Glasgow, UK*
[2] *McDermott International, W4 5XT London, UK*

ABSTRACT

In this study, an alternative modelling approach for absorbed hydrogen stress corrosion cracking (SCC) is proposed, with hydrogen-enhanced decohesion (HEDE) identified as the key failure mechanism. All analyses have been performed by utilising only ABAQUS standard elements, COH2D4T and CPE4T, already available within the software and without the need to develop external subroutines. The study also tends to highlight the criticality of implementing a correct Traction Separation Law (TSL) curve to simulate the hydrogen diffusion within the specimen and using the concept of dynamic hydrogen penetration by continuously updating the hydrogen concentration boundary conditions as the crack propagates. In conclusion, this study successfully demonstrated that standard software elements (COH2D4T and CPE4T) can effectively model physical problems and crack velocity propagation without custom subroutines. It emphasized that while the specific shape of the Traction-Separation Law (TSL) is less critical, its correct implementation is vital for simulating dynamic hydrogen coverage. Crucially, excluding this dynamic coverage—a common practice—risks significantly underestimating crack propagation speed. Although results incorporating dynamic coverage aligned well with experimental data, minor discrepancies are likely due to unmodeled factors like material property variations, hydrogen trapping, temperature, and granular microstructure, which are proposed for future research.

Keywords: Hydrogen Embrittlement; Finite Element Method; Cohesive Zone Model; Stress Corrosion Cracking; Fracture

*CORRESPONDING AUTHOR:
Selda Oterkus, Department of Naval Architecture, Ocean and Marine Engineering, University of Strathclyde, G4 0LZ Glasgow, UK; McDermott International, W4 5XT London, UK; Email: selda.oterkus@strath.ac.uk

ARTICLE INFO
Received: 10 August 2025 | Revised: 17 November 2025 | Accepted: 24 November 2025 | Published Online: 24 December 2025
DOI: https://doi.org/10.36956/sms.v7i4.2617

CITATION
Gravina, D., Oterkus, S., Oterkus,E., 2025. Finite Element Modelling of Hydrogen Embrittlement by Considering Hydrogen Coverage Boundary Conditions. Sustainable Marine Structures. 7(4): 233–254. DOI: https://doi.org/10.36956/sms.v7i4.2617

1. Introduction

Hydrogen power is a key focus in the global shift toward sustainable energy due to its high benefit from environmental point of view and energy density, as it produces no harmful emissions [1,2]. For hydrogen to achieve widespread commercial use, efficient transportation methods are essential. One cost-effective approach for large-scale hydrogen distribution is injecting it as mixture with natural gas (i.e., blending) into existing natural gas pipelines [3,4]. Nevertheless, this method (blending) presents a significant challenge: hydrogen embrittlement (HE). When hydrogen concentrations rise, pipeline steel can lose ductility, increasing the risk of cracks and structural failures.

In late 2020, the UK government introduced its Green Industrial Revolution, made by a Ten-Point Plan, this plan featured several key initiatives. Among these was a focus on hydrogen energy, with the goal of collaborating with industries to achieve 5GW of low-carbon hydrogen production by 2030. This initiative aims to support sectors such as transport, power generation, and residential heating. Additionally, the plan includes an ambitious target to establish the first fully hydrogen-powered town by 2030.

With those points in mind, it is interesting to consider how the existing infrastructure in the UK Continental Shelf (UKCS) can potentially provide support to achieve the above points and the overall government net zero target.

As noted in studies [5,6], the UK Continental Shelf (UKCS) contains more than 250 offshore platforms and an extensive pipeline network spanning approximately 45,000 kilometres. With many of these assets approaching the end of their operational lifespan, oil and gas companies have been actively developing strategies to decommission them in a cost-efficient manner. Consequently, repurposing or extending the service life of existing offshore pipelines has become a key focus. Extensive research has been and continues to be carried out to investigate how hydrogen exposure affects the structural integrity of steel pipelines.

Hydrogen embrittlement (HE), sometimes referred to as hydrogen-induced cracking (HIC) or hydrogen-assisted fracture, is a phenomenon where the absorption of hydrogen by a metal reduces its ductility. Due to their tiny size, hydrogen atoms can diffuse into metallic structures, weakening the material and decreasing the stress needed for crack formation and growth. This process leads to a loss of toughness, making the metal more prone to brittle failure. While HE is particularly common in steels, it can also affect other metals, including nickel, iron, cobalt, titanium, and their respective alloys.

Hydrogen embrittlement can lead to material failure even when steel is subjected to non-cyclical loads. Specifically, stress corrosion cracking (SCC) occurs as a gradual breakdown of the material, caused by sustained tensile stress (rather than cyclic stress) combined with exposure to certain liquid or gaseous environments [7].

The earliest instances of catastrophic stress corrosion cracking (SCC) failures date back to the early 1800s, with numerous boiler explosions resulting in significant loss of life. Initial scientific recognition of this phenomenon came in 1873, when Johnson identified it through laboratory experiments [8]. Despite extensive research and considerable resources invested in studying SCC, devastating failures continue to occur, highlighting the need for further investigation to better comprehend this particular failure mechanism.

Hydrogen embrittlement (HE) causes a multifaceted deterioration process in metallic materials, involving both mechanical and physicochemical interactions. Studies indicate that hydrogen exposure alters fracture behaviour, shifting it from ductile mechanisms—such as micro void coalescence (MVC)—in hydrogen-free conditions to brittle fracture modes, including quasi-cleavage (QC), intergranular (IG), and trans granular (TG) fractures, when hydrogen is present [9,10].

Several classical theories have been established to explain the hydrogen embrittlement (HE) mechanism, with three being the most widely recognized. The first is the hydrogen-enhanced decohesion (HEDE) model [11–14], which proposes that hydrogen atoms penetrating the steel lattice induce expansion and decrease surface energy, weakening atomic bonds. The second theory, referred to as the hydrogen-enhanced localized plasticity (HELP) mechanism [15–18], proposes that hydrogen in solution promotes dislocation motion, reduc-

ing the effective yield strength and enhancing localized plastic deformation, even under low stress or minimal stress intensity. The third model, termed the adsorption-induced dislocation emission (AIDE) mechanism [14–18], postulates that hydrogen aids in dislocation nucleation and propagation, leading to critical failure conditions where crack initiation and growth result from hydrogen-assisted damage.

A recent study by Djukic and colleagues [19] suggests that hydrogen embrittlement (HE) results from the combined influence of the HELP and HEDE (Hydrogen-Enhanced Decohesion) mechanisms, along with their synergistic interaction. Current research indicates that none of the three major theories alone can fully explain the HE phenomenon. Instead, varying mechanical conditions may align with different theoretical models [20].

In recent years, numerical simulation has gained increasing recognition as a valuable approach for hydrogen embrittlement (HE) analysis. Combining experimental data with numerical modelling can significantly enhance the overall understanding of hydrogen-steel interactions. Researchers such as Sofronis and McMeeking [21], Krom et al. [22] and Taha and Sofronis [23], and have contributed to advancing numerical frameworks that integrate hydrogen diffusion with mechanical response.

Cohesive zone modelling (CZM) [24] has gained considerable attention as an effective method for studying material failure. Previous research has explored the interaction between hydrogen diffusion in metals and CZM by incorporating hydrogen-induced degradation laws. To integrate hydrogen-related mechanisms into numerical simulations, several studies have employed quantum mechanics and first-principles calculations to examine hydrogen's role in weakening atomic bonds. For instance, Jiang and Carter [25] used periodic density functional theory to demonstrate that the ideal fracture energy declines nearly linearly with higher hydrogen coverage. Similarly, Serebrinsky et al. [26] developed a computational model to assess hydrogen-assisted damage in high-strength steel, aligning their findings with experimental data under the hydrogen-enhanced decohesion (HEDE) mechanism. Additionally, Sobhaniaragh et al. [27] introduced a fully coupled framework combining hydrogen diffusion and elastoplastic deformation within CZM to simulate hydrogen-induced cracking in high-strength steels.

Modelling hydrogen-induced fracture involves intricate computational steps, such as analysing transient hydrogen diffusion, which depends on determining the stress-strain response of elastic-plastic materials. Additionally, the influence of hydrogen-induced material degradation on fracture behaviour must be integrated into the cohesive zone model (CZM) Therefore, investigating hydrogen embrittlement requires a combined approach using experimental studies and finite element simulations.

Hydrogen embrittlement (HE) remains a critical challenge in structural integrity, particularly for high-strength metals used in aerospace, automotive, and energy industries. Despite decades of research, existing HE models still exhibit significant deficiencies in accurately predicting material failure under hydrogen environments. These shortcomings arise from the complex interplay between hydrogen diffusion, microstructural interactions, and mechanical loading, which current models often oversimplify. As per above, traditional approaches, such as phenomenological fracture criteria and decoupled diffusion-mechanics models, fail to capture the synergistic effects of hydrogen-enhanced localized plasticity (HELP), hydrogen-enhanced decohesion (HEDE), and dislocation-hydrogen interactions. Moreover, most models lack predictive capabilities across different material systems and loading conditions, limiting their applicability in engineering design.

The importance of advancing HE research lies in ensuring the safe deployment of hydrogen-based technologies, such as fuel cells and hydrogen storage systems, where material failure can have catastrophic consequences. Additionally, the growing use of high-strength alloys in extreme environments (e.g., deep-sea pipelines, nuclear reactors) necessitates accurate HE prediction tools to prevent premature failures. Improved models could also aid in alloy design, enabling the development of HE-resistant materials through computational screening.

Recently a number of studies have been conducted to analyse the effect of hydrogen embrittlement on

material behaviour and the key modern trends in HE modelling are: Multi-Scale Integration: Linking quantum/atomistic insights to macroscopic component performance [28,29]; Coupled Diffusion-Stress Modelling: Simulating how stress fields and plastic deformation influence hydrogen transport and trapping [30,31]; Machine Learning (ML): Using data-driven approaches to predict HE susceptibility and identify critical parameters [32]; and finally Focus on Specific Microstructural Features: Explicitly modelling grain boundaries, precipitates, and phase interfaces [33–35].

This study aims to model hydrogen-induced brittle fracture using conventional ABAQUS elements. A two-dimensional plane strain element was utilized to analyse hydrogen-assisted fracture behaviour through a two-stage process involving stress evaluation, hydrogen diffusion assessment, and cohesive zone stress analysis under hydrogen influence. The cohesive zone model (CZM) incorporated a bilinear traction-separation law (TSL), with an additional examination of how hydrogen concentration affects TSL degradation. The key innovations and findings of this research include:

- Novel Simulation Approach: Development of a new technique to model hydrogen embrittlement using ABAQUS standard elements (COH2D4T and CPE4T).
- Cohesive Element Analysis: Assessment of cohesive element efficiency and the impact of TSL geometry on model performance.
- Advanced Hydrogen Diffusion Modelling: Implementation of a specialized algorithm designed to:
    - Track the evolving crack tip location.
    - Apply saturated hydrogen coverage along newly formed crack surfaces
    - This process replicates the infiltration of aqueous solutions into the material as the crack propagates—a critical aspect overlooked in existing literature.

In summary, the main novelty of the proposed study is to demonstrate the capability of ABAQUS standard software elements (COH2D4T and CPE4T) to effectively model the physical problem and crack velocity propagation without custom subroutines. Moreover, the effect of Dynamic Hydrogen Coverage (DHC) is considered to accurately represent hydrogen diffusion as the crack propagates.

2. Materials and Methods

This research investigates hydrogen embrittlement through a fully coupled thermomechanical model, implemented using the finite element software ABAQUS by utilising the analogy between variables in heat transfer and mass diffusion. Hydrogen transport is typically modelled using diffusion equations derived from a phenomenological framework, where material domain fluxes and mass conservation principles are applied [36]. As discussed earlier, hydrogen atoms contribute to material degradation by weakening atomic bonds, influencing dislocation behaviour, and altering mechanical properties.

Furthermore, hydrogen diffusion is affected by the stress-strain field, primarily through two key factors: hydrostatic stress and plastic strain. Hydrostatic stress induces lattice expansion, driving hydrogen atoms toward dilated regions, while plastic strain generates crystal defects that act as trapping sites for hydrogen. This interaction is particularly significant near crack tips, where plastic strain becomes highly concentrated. Due to these mechanisms, hydrogen diffusion models often adopt a dual-phase approach, treating trapped and lattice hydrogen as distinct chemical species.

This research follows widely accepted assumptions in the field, with the model grounded in the equilibrium framework established by Oriani [37]. In this context, the notation L denotes lattice sites, while T represents trap sites. A key assumption is that trap sites are isolated, meaning they do not interconnect to form a continuous network. Consequently, hydrogen diffusion between trap sites occurs primarily through lattice diffusion.

The hydrogen effect on the cohesive elements is considered by modifying the TSL based on hydrogen concentration. To this intent, the hydrogen coverage parameter is introduced and defined as:

$$\psi = \frac{SHC}{SHCSV}, \tag{1}$$

where represents the surface hydrogen concentration at the crack tip, while denotes the saturation value of the surface hydrogen concentration.

To accurately assess the reduction in material strength caused by hydrogen localization and its impact on fracture mechanics, it is essential to couple the diffusion and mechanical fields. Hydrogen adsorption and its migration along grain boundaries can induce localized embrittlement, altering the material's behaviour under mechanical loading. According to Lynch [8], this process can be attributed to the hydrogen absorption-induced decohesion (AIDEC) mechanism, which reduces interatomic bonding strength and promotes localized fracture.

The methodology used in this research extends the impurity-dependent cohesive zone model developed by Serebrinsky [26], which was derived from first-principle computational analyses. The governing equation for this model, as presented in Serebrinsky's study [26], is expressed as follows:

$$k = \frac{\sigma_c(\psi)}{\sigma_c(0)} = 1 - 1.0467\psi + 0.1687\psi^2, \qquad (2)$$

In other words, the original critical stress for the cohesive elements is inversely proportional to the local hydrogen concentration in the specimen. The proposed numerical methodology consists of the following key steps:

1. Mechanical Loading Phase
    - The specimen is subjected to a displacement-controlled load on its upper and lower surfaces until the desired stress intensity factor is reached.
    - This load is maintained constant until crack initiation occurs.
2. Hydrogen Coverage Initialization
    - A hydrogen coverage at saturation (unit value) is applied exclusively at the crack tip.
    - Hydrogen coverage is set to zero on all other specimen surfaces.
3. Hydrogen Diffusion Analysis
    - A diffusion model, derived from an analogy with the heat equation, predicts hydrogen distribution along grain boundaries at each computational time step.
4. Material Embrittlement Evaluation
    - The local hydrogen concentration's impact on material strength is quantified using Equation (16).
5. Dynamic Crack Propagation and Coverage Update
    - A dedicated algorithm performs two critical functions:
        - Tracks the advancing crack tip and updates its position accordingly.
        - Introduces a uniform hydrogen layer to the newly created crack faces.
    - This step simulates the infiltration of aqueous solution into the material during crack propagation, as referenced in [26].

3. Results

To validate and demonstrate the capability of the current approach, two different configurations were considered, including a two-dimensional plate and a pre-cracked thin steel plate under tension loading.

3.1. Validation Case

The first numerical example is a validation case to test the proposed approach by considering a two-dimensional plate with dimensions of 0.1x0.11m. The FEM is presented in **Figure 1**. The model consists of Bidimensional 4-node cohesive elements (COH2D4T) with displacement and temperature degrees-of-freedom (DOF) in conjunction with 4-node plane strain thermally coupled quadrilateral elements (CPE4T) with displacement and temperature DOF. The cohesive elements are placed at the location of a possible crack. Cohesive elements have two Gauss points, whereas the 4-node plane strain continuum elements have 4(four) integration points.

The finite element model consists of ten cohesive elements (series 5000 in **Figure 1**) and one hundred continuum elements placed symmetrically on both sides of the ten cohesive elements (series 100, 200, 300, ..., 1000 in **Figure 1**). For simplicity, the cohesive and continuum elements have the same dimensions.

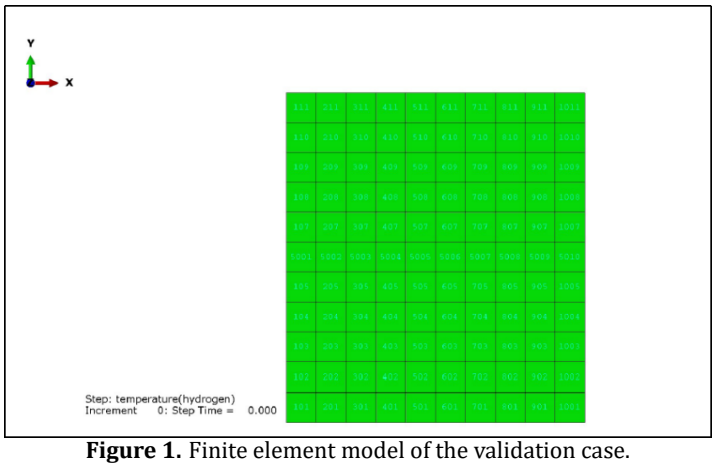

Figure 1. Finite element model of the validation case.

The applied load is constant and uniaxial (mode I test). The simulation is run under displacement control, applying the same displacement to the 11 upper and bottom nodes of the continuum elements. The material of the continuum elements is a linear elastic material with Young's Modulus of 205,000 MPa, Poisson's ratio of 0.3 and Diffusivity of 0.00084 mm^2/s. The constitutive law of the cohesive element is defined as elastic for the initial slope of the TSL, maximum stress for the damage initiation criterion, and displacement-type linear softening behaviour for damage evolution. All TSL parameters have been defined as a function of the concentration of hydrogen, which is the temperature variable in ABAQUS, based on the analogy between thermal diffusion and hydrogen diffusion considered in this study.

3.1.1. Cohesive Elements in the Presence of Hydrogen

In this case, the sample is pre-charged for a specific value of hydrogen concentration for which the corresponding values of and have been calculated. The analysis then runs only one step, for which the following boundary conditions are applied:

- 1st step: same displacement (0.006 mm) is applied to the 2 x 11 upper and bottom nodes of the continuum elements.

Figure 2 summarises the results for four tests performed for different hydrogen concentrations for which the corresponding values of and have been calculated. For clarity, all four tests were carried out without and with the presence of hydrogen, (which corresponds to sample charged to saturated level of hydrogen) and TSL curves were reconstructed from the analysis. As can be in this figure, TSL curves are different for different concentrations of hydrogen which are degrading as the hydrogen concentration changes.

These results demonstrate that our model can accurately reproduce the TSLs in accordance with the input data which describe the presence of hydrogen at various concentration levels within the sample.

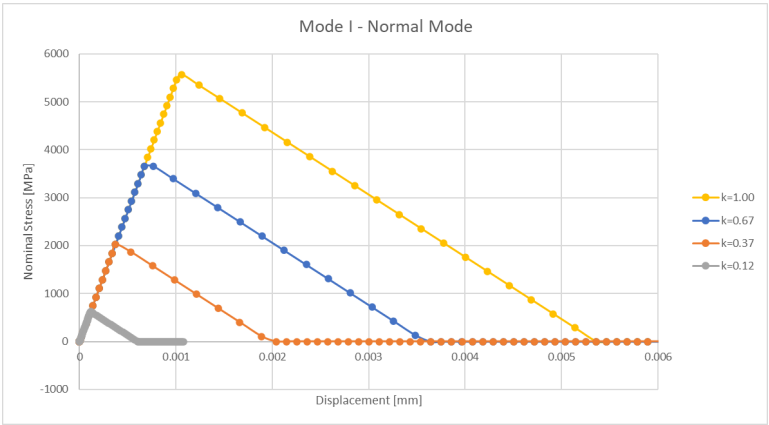

Figure 2. TSL curves for different hydrogen concentration values.

3.1.2. Sample Charged with Hydrogen without Dynamic Coverage

In this case, the initial condition of the sample is without presence of hydrogen. The analysis was then performed in two steps, in which the following boundary conditions were applied:

- 1st step: same displacement (0.0017 mm) is applied to the 2 x 11 upper and bottom nodes of the continuum elements.
- 2nd step: the saturation concentration of hydrogen (2.650×10^{-11} mol/mm^2) is applied to the four nodes of Element ID 5001 (please refer to **Figure 1**)

Figures 3–6 show results for the hydrogen concentration and cohesive degradation at various time intervals. As can be seen in the figures, the hydrogen saturation concentration is applied only to the four nodes of Element ID 5001 (please refer to **Figure 1**), and while the hydrogen gets diffused within the sample, at constant load, various cohesive elements reach full degraded status, i.e., SDEG parameter reaches 1.00 for a growing number of cohesive elements. Note that hydrogen boundary conditions do not change regardless of the degradation of the CZM.

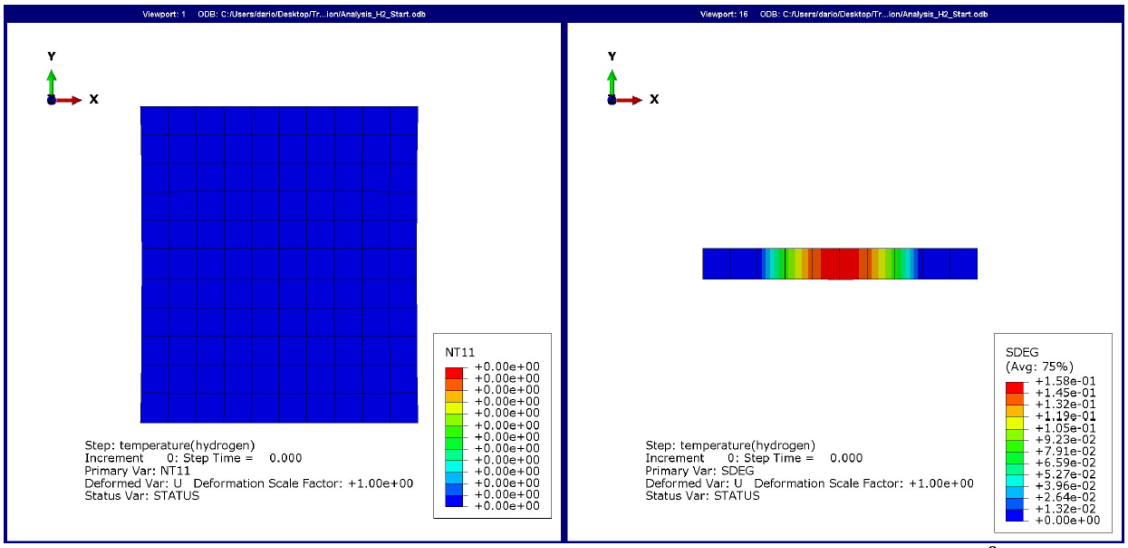

Figure 3. Simulation without Dynamic Hydrogen Coverage: Hydrogen concentration (NT11 [mol/mm^2]), cohesive element degradation (SDEG [-]) at step time 0.000sec. (before applying hydrogen).

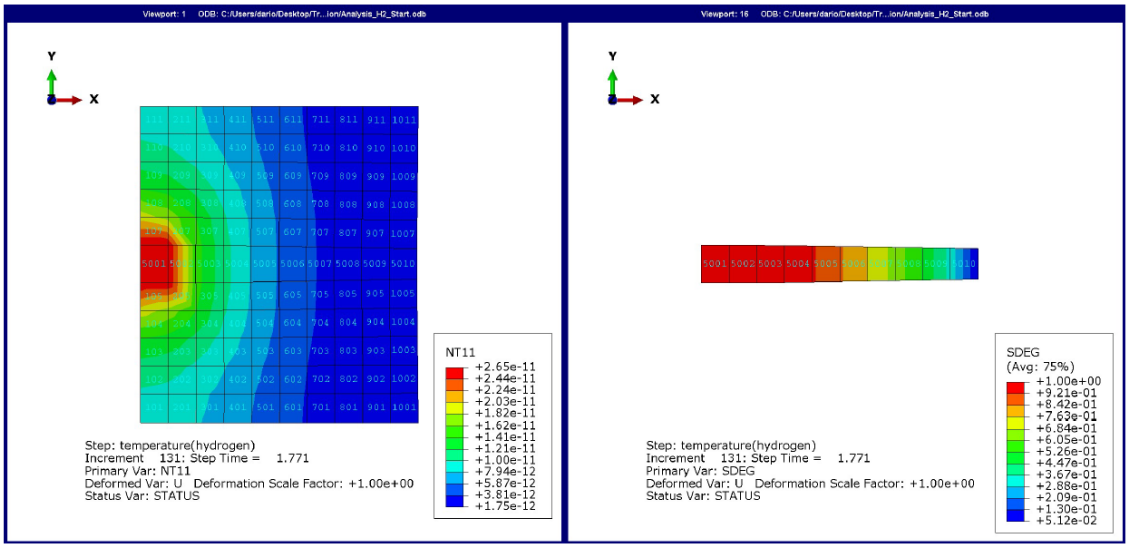

Figure 4. Simulation without Dynamic Hydrogen Coverage: Hydrogen concentration (NT11 [mol/mm^2]), cohesive element degradation (SDEG [-]) at step time 1.771 sec. (Element 5003 fully degraded).

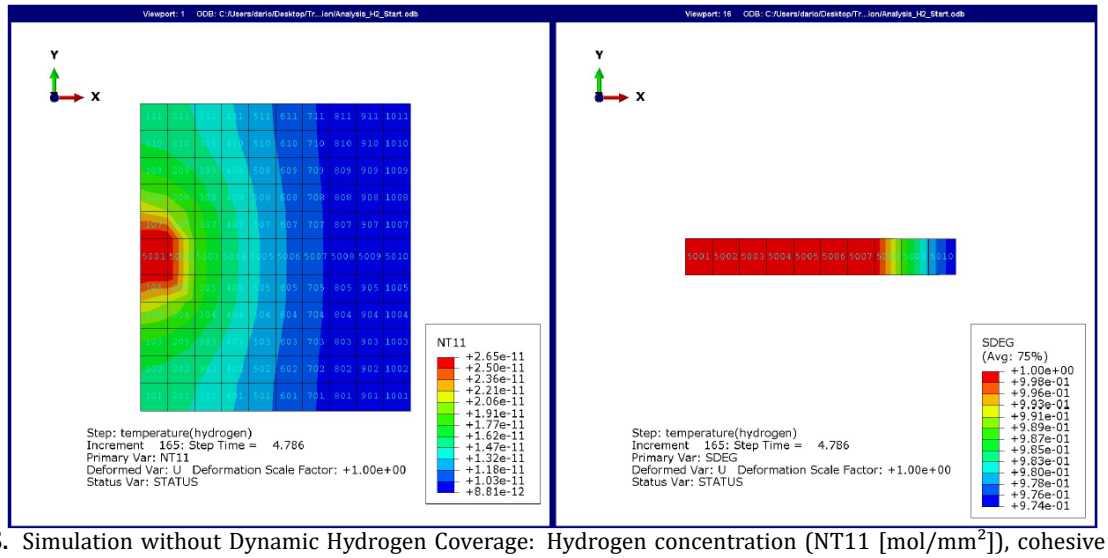

Figure 5. Simulation without Dynamic Hydrogen Coverage: Hydrogen concentration (NT11 [mol/mm^2]), cohesive element degradation (SDEG [-]) at step time 4.786 sec. (Element 5007 fully degraded).

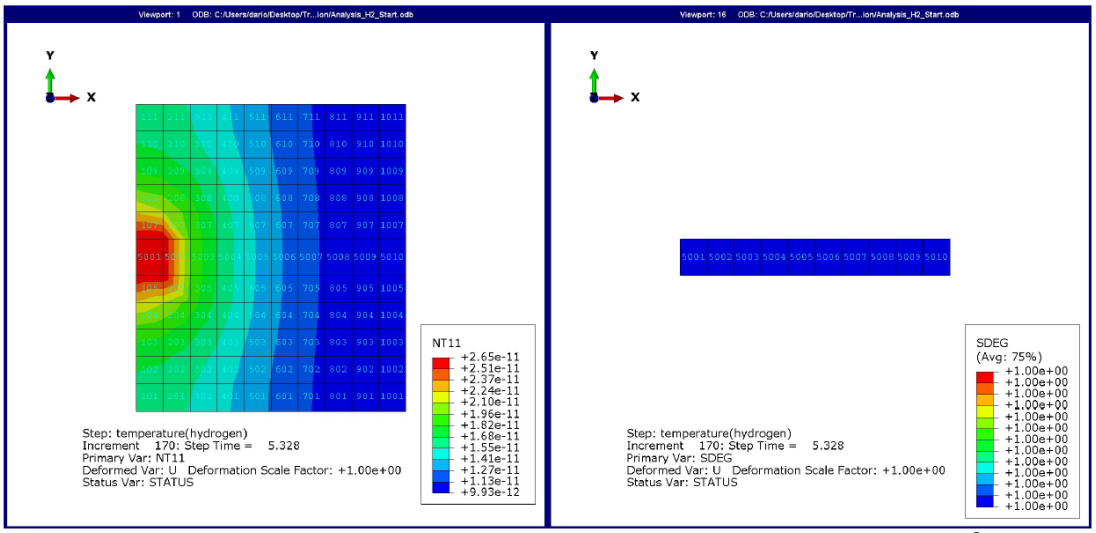

Figure 6. Simulation without Dynamic Hydrogen Coverage: Hydrogen concentration (NT11 [mol/mm^2]), cohesive element degradation (SDEG [-]) at step time 5.328 sec. (All Cohesive Elements are fully degraded).

3.1.3. Sample Charged with Hydrogen by Considering Dynamic Coverage

This study investigates the dynamic effects of hydrogen coverage during crack propagation. Specifically, a novel algorithm is designed to:

- identify the updated crack tip location, and
- assign a unit hydrogen coverage value to the newly formed crack surfaces.

The approach simulates how an aqueous solution infiltrates the material as the crack extends.

For clarity, the sample having the same geometrical and loading characteristics as in the previous case has been considered in this case. **Figures 7–10** show results for the hydrogen concentration and cohesive degradation at various time intervals. As shown in these figures, the hydrogen saturation concentration penetrates within the sample, and while the hydrogen gets diffused within the sample at constant load, various cohesive elements reach a fully degraded status (SDEG parameter reaches 1.00 for a growing number of cohesive elements).

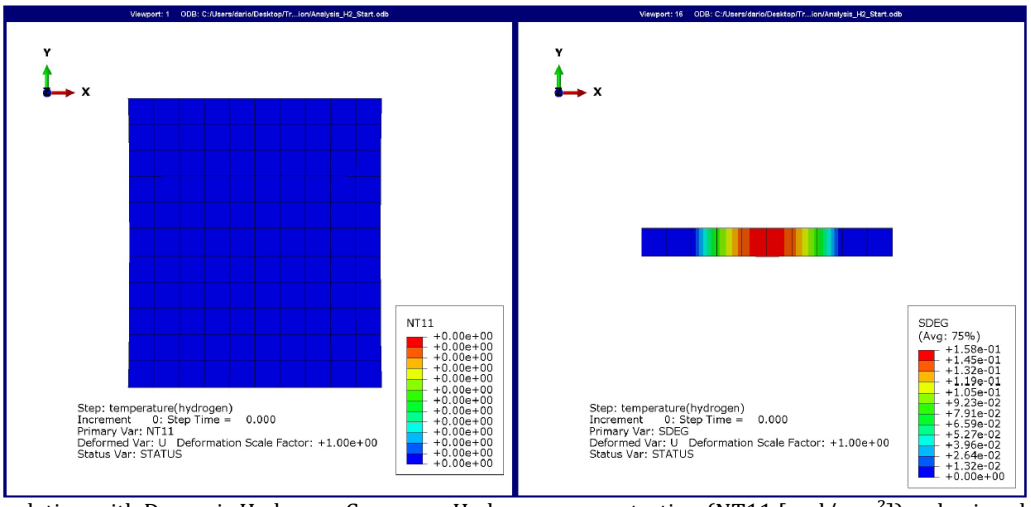

Figure 7. Simulation with Dynamic Hydrogen Coverage: Hydrogen concentration (NT11 [mol/mm^2]), cohesive element degradation (SDEG [-]) before applying hydrogen.

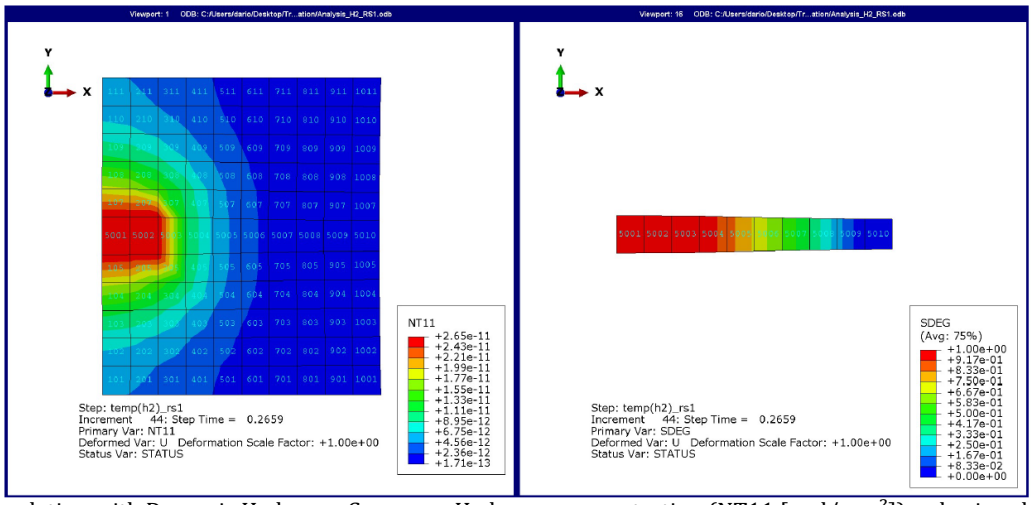

Figure 8. Simulation with Dynamic Hydrogen Coverage: Hydrogen concentration (NT11 [mol/mm^2]), cohesive element degradation (SDEG [-]) when Element 5003 is fully degraded.

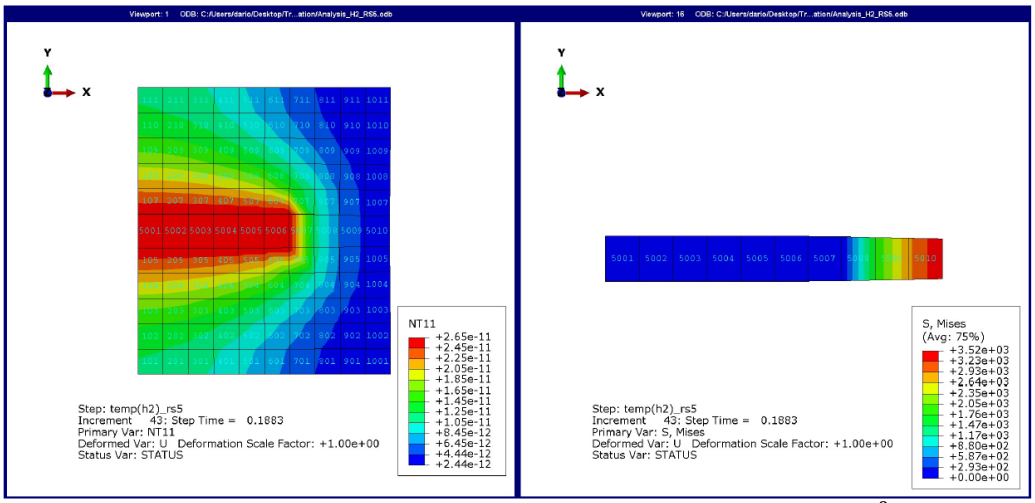

Figure 9. Simulation with Dynamic Hydrogen Coverage: Hydrogen concentration (NT11 [mol/mm^2]), cohesive element degradation (SDEG [-]) when Element 5007 is fully degraded.

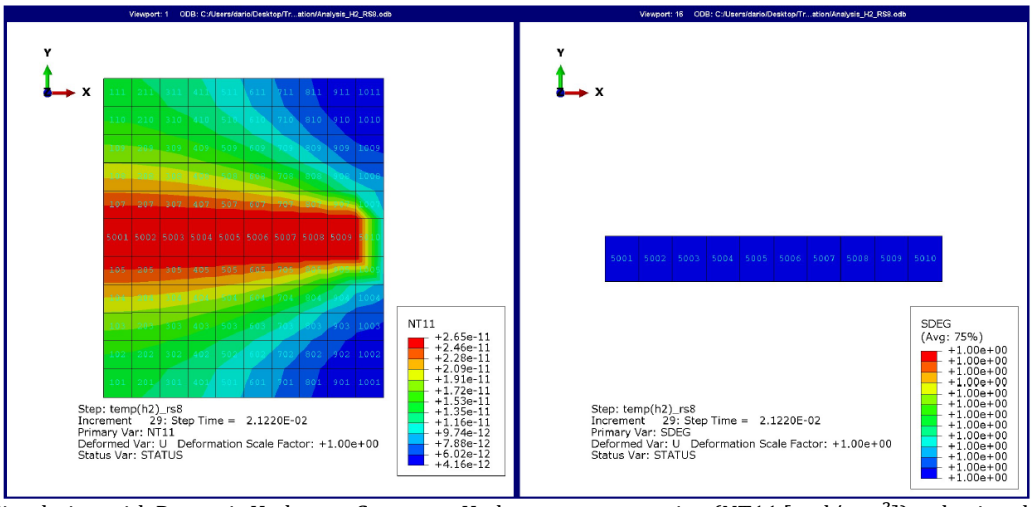

Figure 10. Simulation with Dynamic Hydrogen Coverage: Hydrogen concentration (NT11 [mol/mm^2]), cohesive element degradation (SDEG [-]) when all Cohesive Elements are fully degraded.

3.1.4. Dynamic Hydrogen Coverage Modelling and Its Effect

As previously mentioned, the approach simulates how an aqueous solution infiltrates the material as the crack extends. In particular, when the computation code evaluates that a specific cohesive element is fully degraded, a new ABAQUS input file is generated as output by a FORTRAN subroutine in ABAQUS and includes the entire script. In the new analysis step, the boundary conditions will reflect the hydrogen coverage to the newly formed crack surfaces. The new input file is then executed by ABAQUS as a restart file, and will initiate the analysis from the last step and iteration from the previous analysis.

In this section, the effect of dynamic hydrogen coverage will be investigated by comparing results obtained in previous cases. The results presented in **Figure 11** show the difference in crack propagation behaviours with and without considering dynamic hydrogen coverage. In particular, the degradation of the sample in the second numerical case is estimated to fully develop in approximately 5.5 seconds. On the other hand, considering the dynamic hydrogen coverage approach the phenomena happen only in less than 2.0 sec. with a difference of more than 150%.

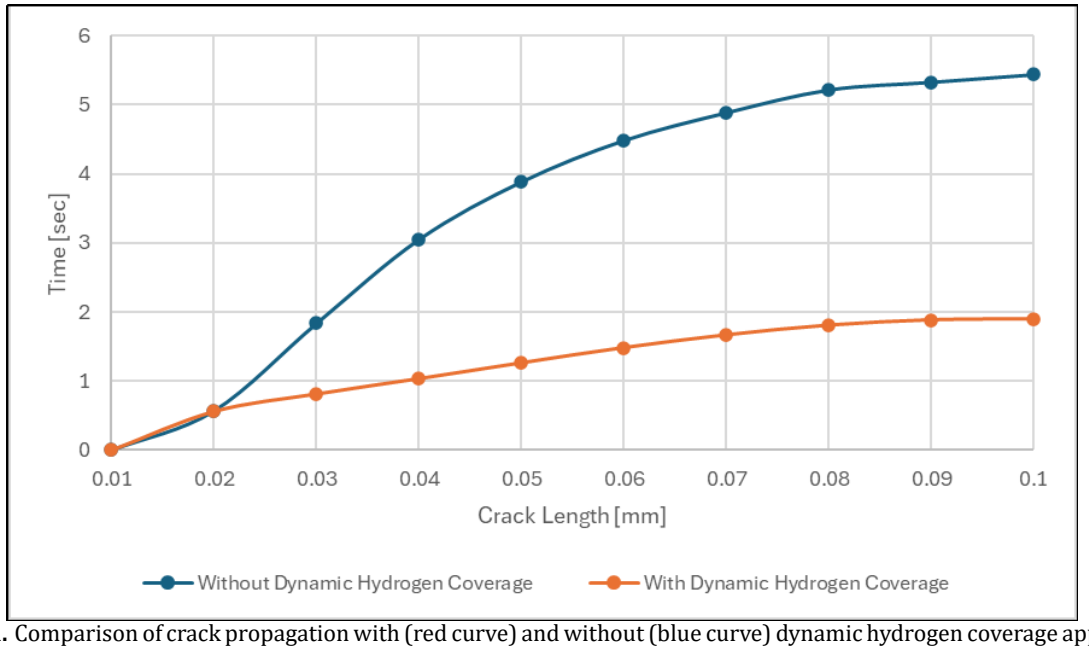

Figure 11. Comparison of crack propagation with (red curve) and without (blue curve) dynamic hydrogen coverage approaches.

3.2. Pre-Cracked Thin Steel Plate under Tension Loading

This numerical study examines a thin steel plate with a pre-existing crack, immersed in a 0.1 N H_2SO_4 aqueous solution. A constant load, applied as a displacement boundary condition, is imposed on the top and bottom edges of the plate. The load magnitude is determined by the stress intensity factor (SIF) and remains fixed throughout the simulation after being statically introduced at the analysis onset. The plate dimensions are as follows: length (L) = 2.0 mm, width (W) = 0.63 mm, and thickness (h) = 5.95 × 10^{-3} mm. The initial crack length measures 1.25 mm.

The vertical displacement-controlled load is applied at a magnitude designed to produce a specific, constant stress intensity factor (SIF) at the crack tip, as outlined in **Table 1**. This initial SIF is kept below the material's fracture toughness to ensure the specimen deforms without initiating crack propagation. **Table 1** provides the five predefined SIF values along with their corresponding displacement loads (u).

Table 1. Relationship between: SIF [$MPa\sqrt{m}$] vs. u [μm].

SIF	13.7	20.6	30.1	40.3	48.55
u	1.157	1.7399	2.5422	3.4	4.1

It is important to note that, along with the vertically enforced displacement, a consistent saturated layer of hydrogen coverage is maintained at the crack tip.

The material AISI 4340 has been considered by assuming a perfect elastic behaviour having a Young's Modulus of 205,000 MPa, Poisson's ratio of 0.3, diffusivity of 0.00084 mm^2/s, and fracture toughness K_{IC} = 58.4 $MPa\sqrt{m}$. TSL curves describe the degradation of the CZM due to an increase in hydrogen concentration are shown in **Figure 12**.

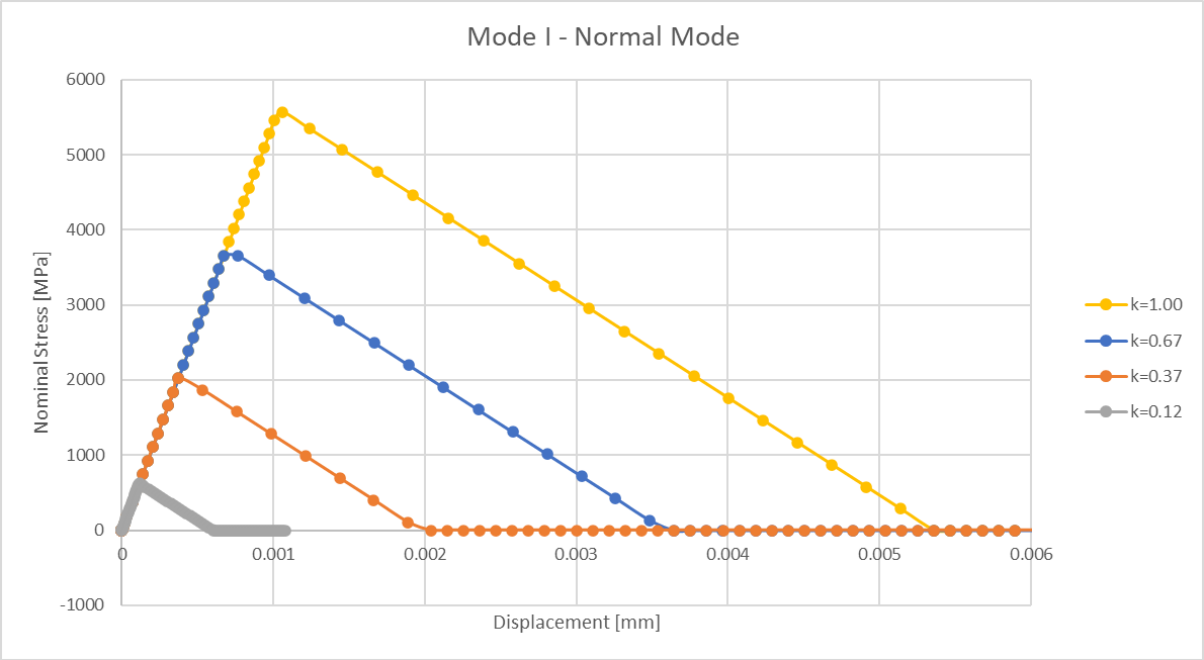

Figure 12. TSL curves for different hydrogen concentration values.

3.2.1. Mechanical Step

The numerical analysis starts with the mechanical step. As expected, during this particular step crack, propagation does not occur at the beginning of the simulation and degradation in CZM due to an increase in hydrogen concentration is required to obtain crack propagation and extension (see **Figure 13**).

Figure 13. Completion of the Mechanical step: Displacement along Y-Axis (U2 [mm]) and cohesive element degradation (SDEG [-]).

3.2.2. Fracture Initiation and Propagation without Dynamic Hydrogen Coverage

In this case, dynamic hydrogen coverage is not considered. Therefore, the location of the applied hydrogen coverage boundary condition doesn't change throughout the analysis. **Figures 14–17** show the diffusion of the hydrogen within the specimen. The red colour identifies the presence of hydrogen at a saturated concentration level (2.650e-11 mol/mm^2) and cohesive elements were fully degraded and not contributing to the resistance of the specimen. As shown in the figures, as the time/analysis progresses, hydrogen diffuses starting from the crack tip region and yields degradation of CZM as presented in **Figure 17**.

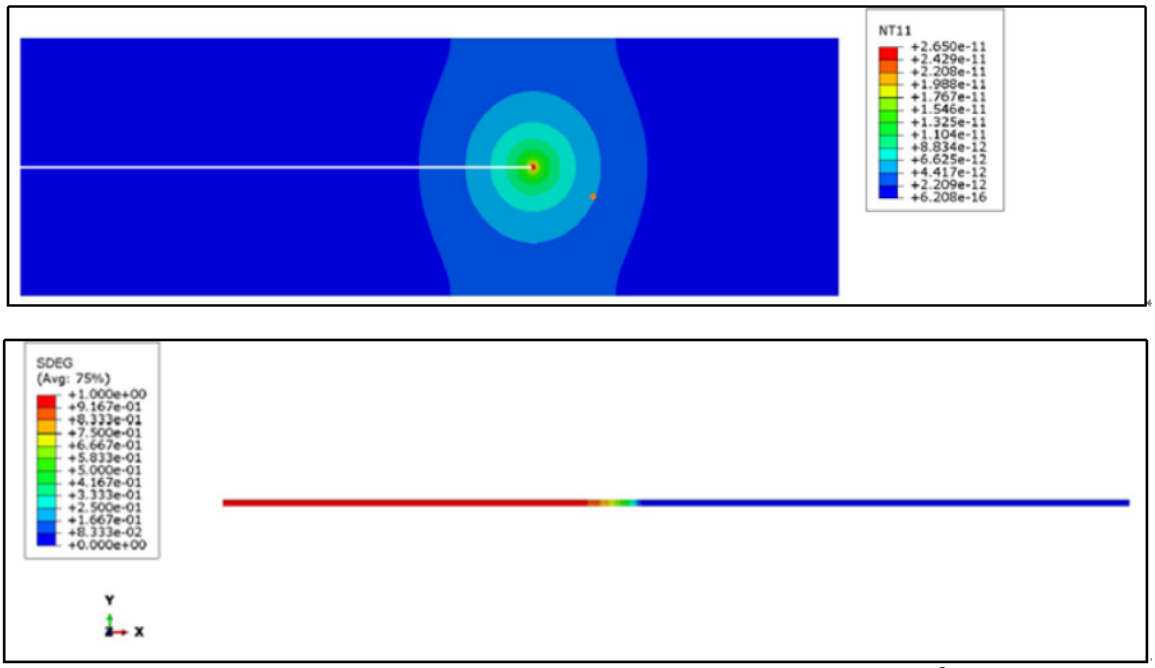

Figure 14. Simulation with Dynamic Hydrogen Coverage: Hydrogen concentration (NT11 [mol/mm^2]), cohesive element degradation (SDEG [-]) at approximately 10 sec.

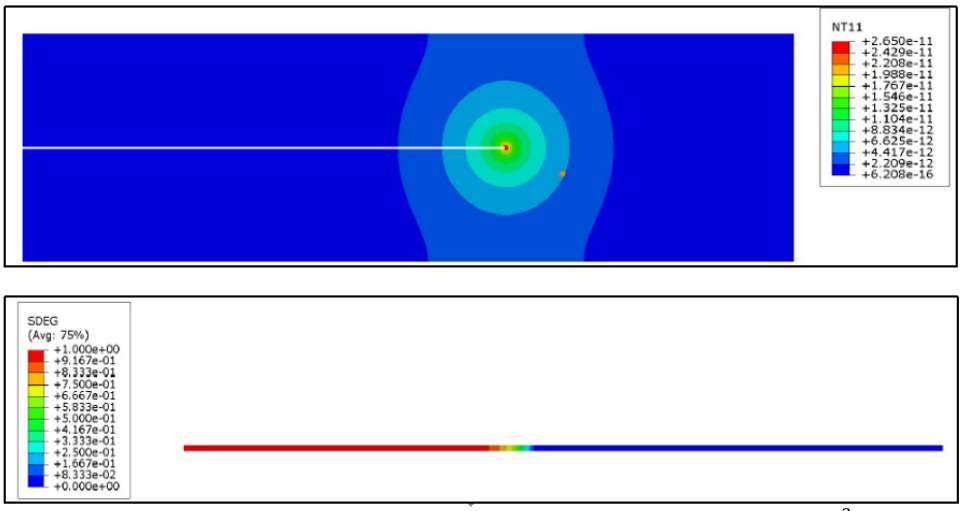

Figure 15. Simulation with Dynamic Hydrogen Coverage: Hydrogen concentration (NT11 [mol/mm^2]), cohesive element degradation (SDEG [-]) at approximately 60 sec.

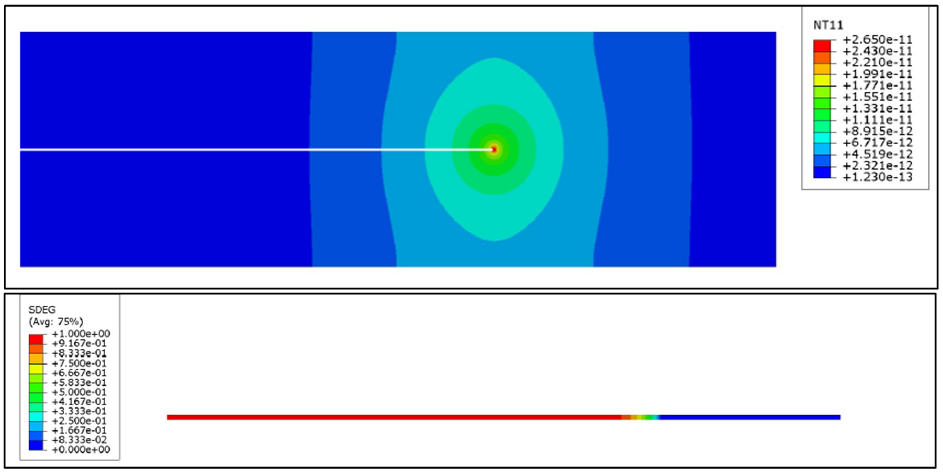

Figure 16. Simulation with Dynamic Hydrogen Coverage: Hydrogen concentration (NT11 [mol/mm^2]), cohesive element degradation (SDEG [-]) at approximately 150 sec.

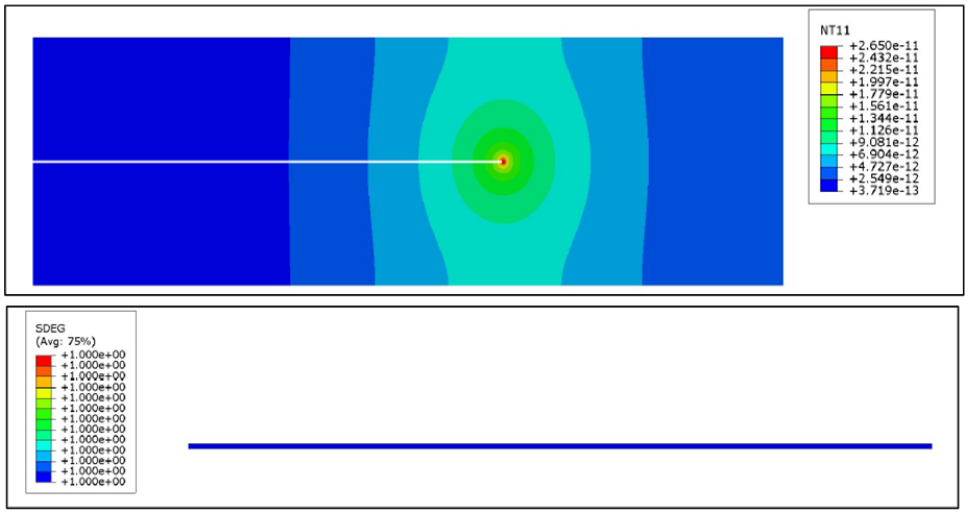

Figure 17. Simulation with Dynamic Hydrogen Coverage: Hydrogen concentration (NT11 [mol/mm^2]), cohesive element degradation (SDEG [-]) at approximately 200 sec (Cohesive Elements fully degraded).

3.2.3. Fracture Initiation and Propagation with Dynamic Hydrogen Coverage

This section examines hydrogen diffusion within the specimen under hydrogen dynamic coverage conditions (see **Figures 18–21**). The boundary condition for hydrogen coverage shifts dynamically in response to crack propagation. Saturated hydrogen concentration (2.650×10^{-11} mol/mm^2) is indicated by the red regions, where cohesive elements have completely degraded and no longer contribute to the specimen's resistance. Unlike the previous scenario, hydrogen spreads inward from the crack tip, causing cohesive zone model (CZM) degradation at a varying rate. Additionally, hydrogen migration follows the crack path, diffusing predominantly toward the rear of the sample rather than the front.

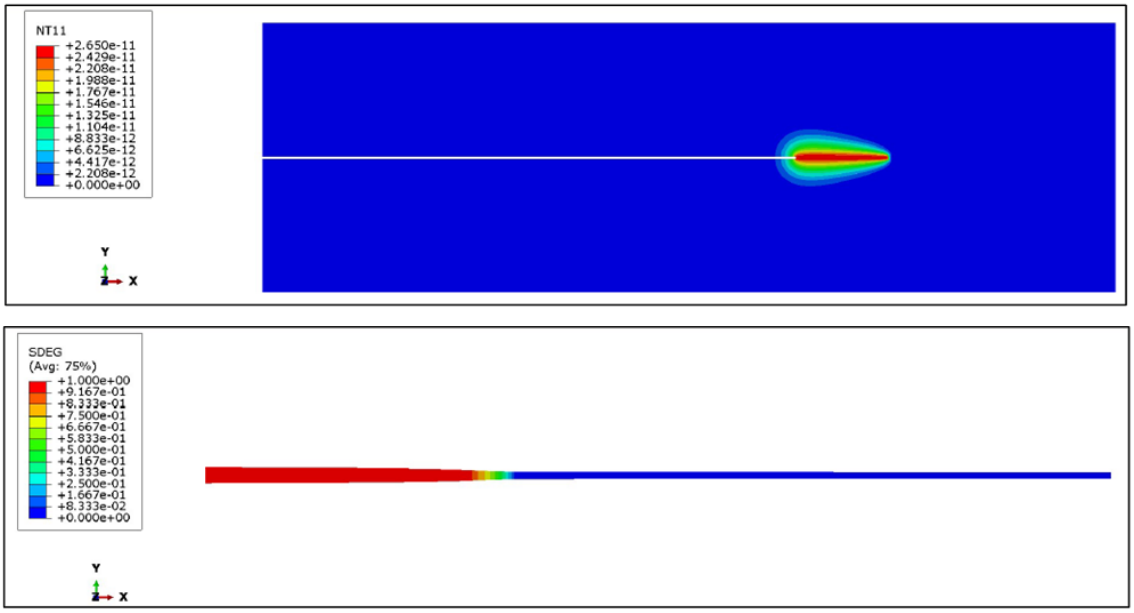

Figure 18. Simulation with Dynamic Hydrogen Coverage: Hydrogen concentration (NT11 [mol/mm^2]), cohesive element degradation (SDEG [-]) at approximately 1 sec.

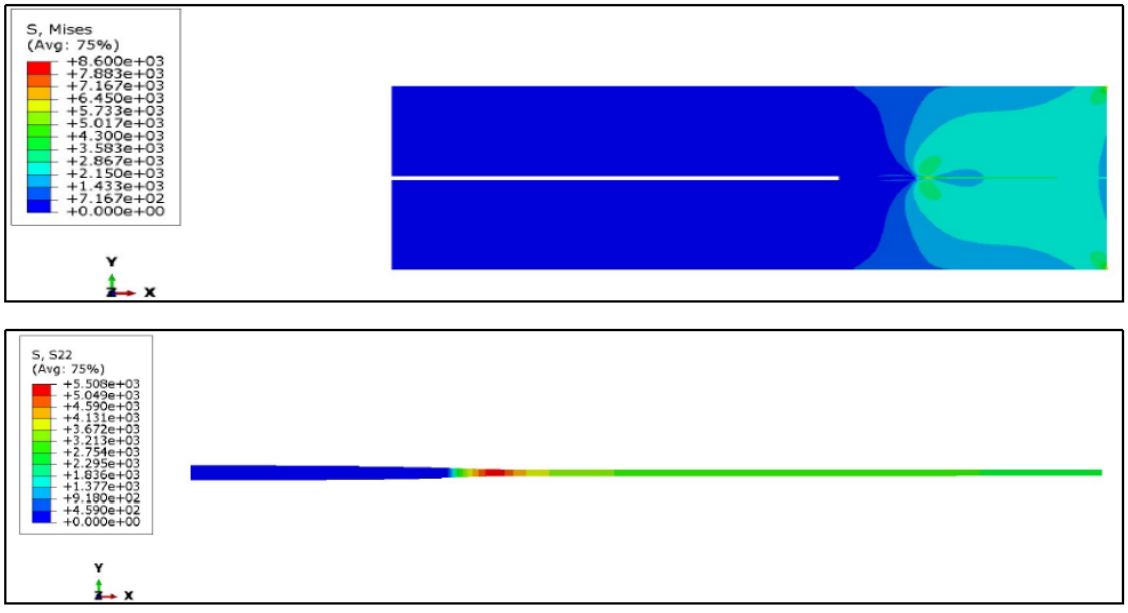

Figure 19. Simulation with Dynamic Hydrogen Coverage: Von Mises Stress (S, Mises [MPa]), cohesive element stress Y axis direction (S22 [MPa]) at approximately 1 sec.

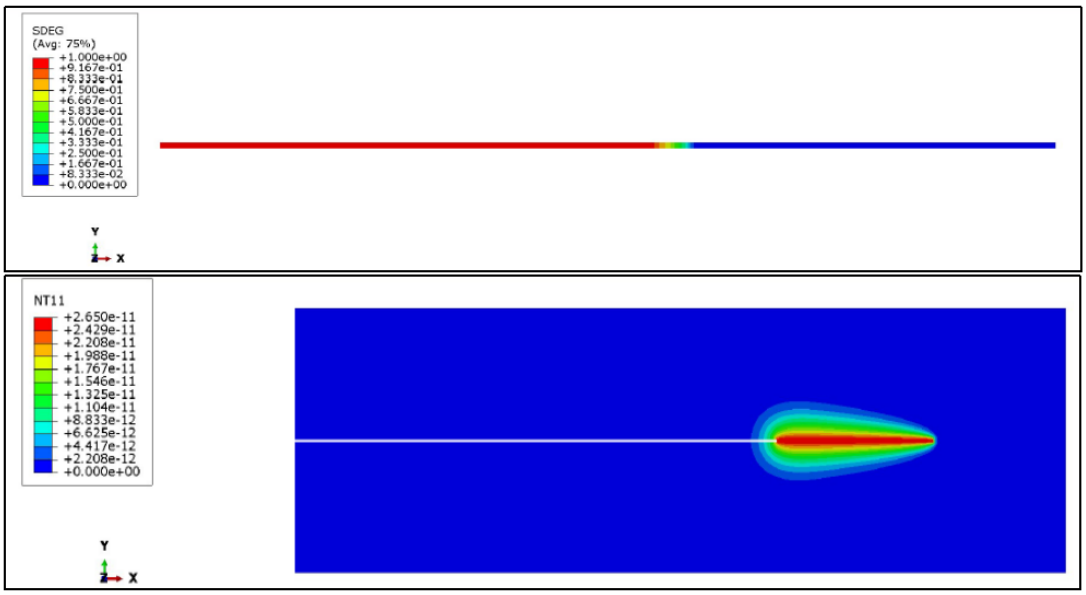

Figure 20. Simulation with Dynamic Hydrogen Coverage: Hydrogen concentration (NT11 [mol/mm^2]), cohesive element degradation (SDEG [-]) at approximately 2 sec.

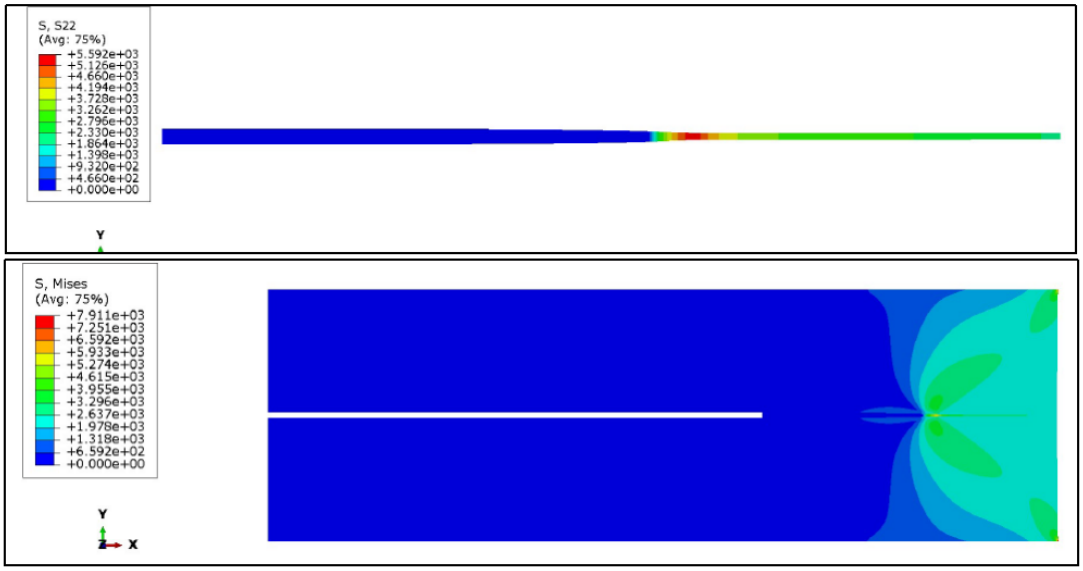

Figure 21. Simulation with Dynamic Hydrogen Coverage: Von Mises Stress (S, Mises [MPa]), cohesive element stress Y axis direction (S22 [MPa]) at approximately 2 sec.

3.2.4. Comparison of the Models with and without Dynamic Hydrogen Coverage against Experimental Data

As discussed in previous sections, the existing model can simulate crack propagation in hydrogen-rich environments using both standard elements and elements with dynamic hydrogen coverage. With and without dynamic hydrogen coverage, crack propagation primarily depends on the material's fracture toughness rather than the Traction Separation Law's shape.

Figures 22–23 highlight the key advantage of incorporating dynamic hydrogen coverage. Specifically, specimen degradation occurs in roughly 25 seconds when dynamic hydrogen coverage is active, compared to approximately 700 seconds without it—a standard assumption in many studies.

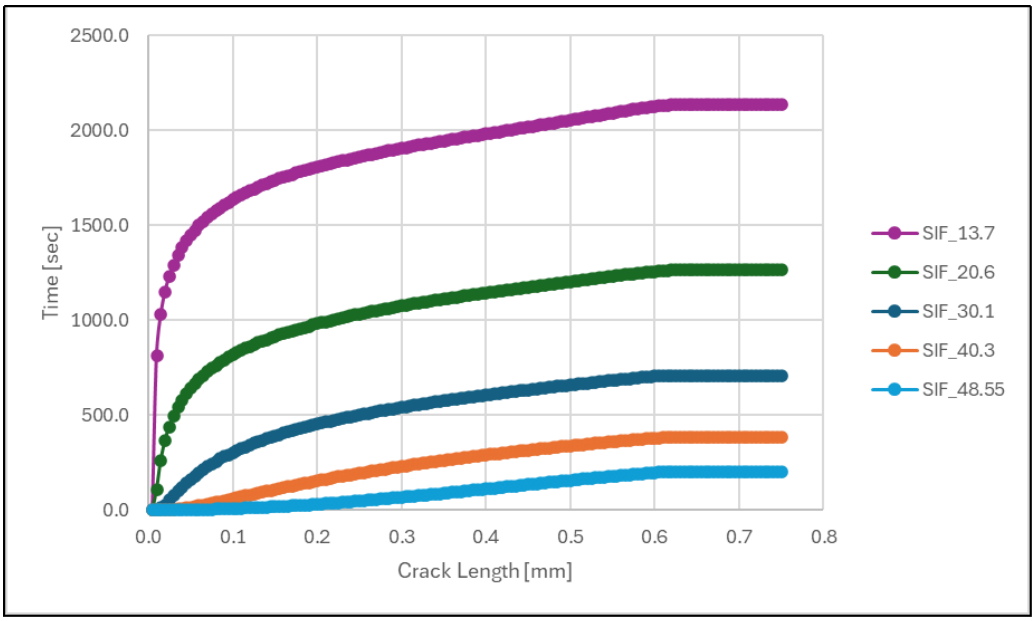

Figure 22. Simulation with Dynamic Hydrogen Coverage: Crack propagation length vs time.

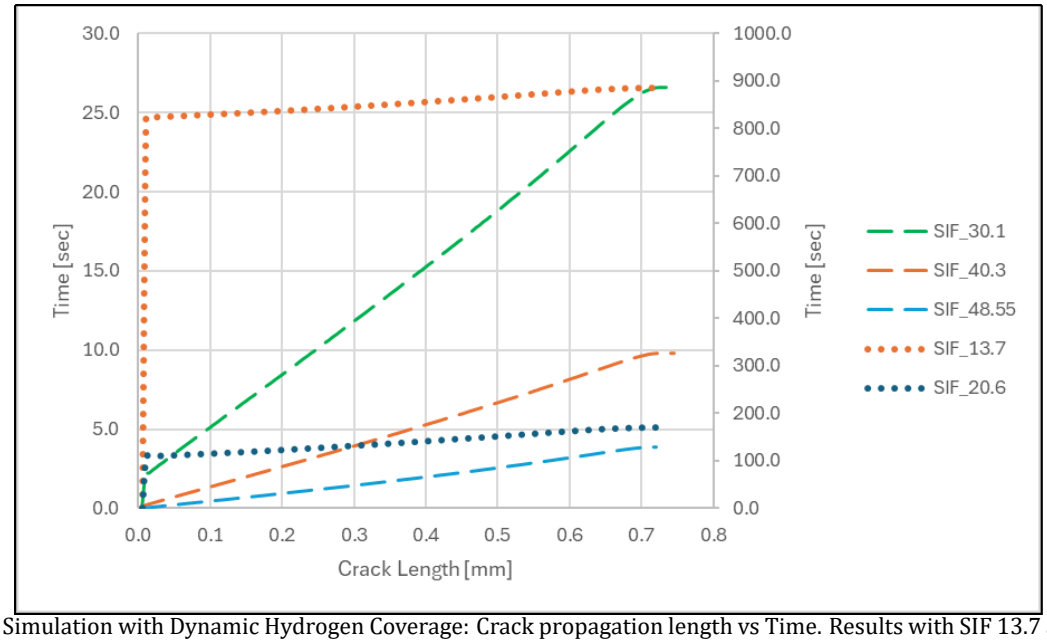

Figure 23. Simulation with Dynamic Hydrogen Coverage: Crack propagation length vs Time. Results with SIF 13.7 and 20.6 are referred to Y-Axis on the right.

Finally, **Figure 24** shows the comparison between the present model with and without dynamic hydrogen coverage and experiments in Hirose and Mura [38,39] concerning the relationship between the crack propagation speed (logarithmic scale) and the stress intensity factor for all five loading conditions. The speed of the crack is calculated for every simulation as the ratio of the crack's total propagation length to its propagation time.

The results clearly indicate the constant risk of underestimating the crack propagation speed if the hydrogen dynamic coverage is excluded in the analysis, as expected. For the analysis, which includes the hydrogen dynamic coverage the numerical results tend to have a good approximation of the experimental data however some differences may be associated to different reasons, such as variation in material properties, the mechanism of the hydrogen trapping, the temperature of the specimen and the granular microstructure, which has not been considered in this study.

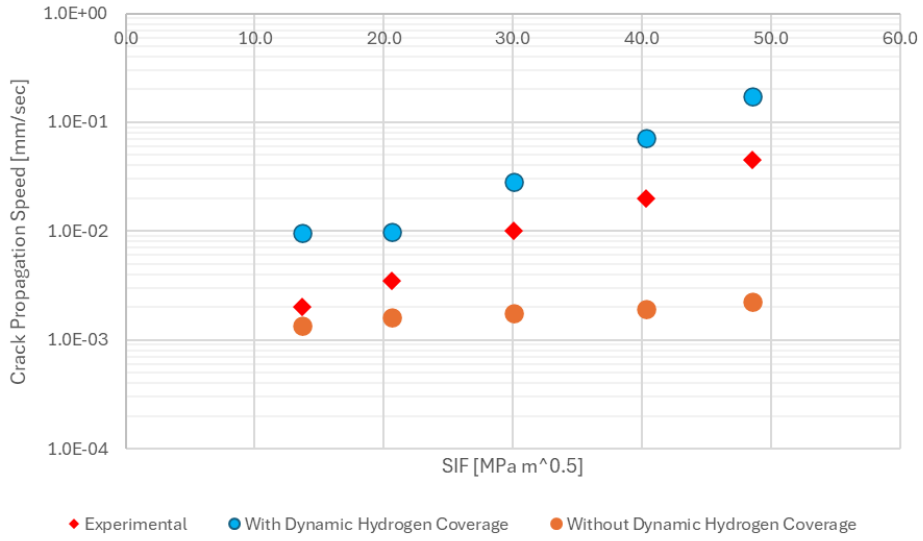

Figure 24. Comparison of the current model with (blue circle) and without (orange circle) dynamic hydrogen coverage approaches against experimental results (red diamond): Crack Propagation speed[mm/s] Vs SIF[MPa √m].

3.2.5. Sensitivity Analysis

Several simulations have been carried out also to validate the correct applicability of the boundary conditions (BCs), the cohesive elements viscosity parameters and the influence of the TSL shape in the overall behaviour of the analysis.

To substantiate the above statement, the numerical convergence of fracture problems in presence of cohesive elements can result in a challenging exercise due to numerical instability associated with the solution of the differential equation in presence of a crack propagation problem. To overcome the above-mentioned problem the utilisation of viscous regularization has been implemented. It is important to clarify that a small value of the viscosity parameter (small compared to the characteristic time increment) has been introduced. This small viscosity usually helps improve the rate of convergence of the model in the softening regime, without compromising results and has been calculated as a result of trial error process [40]. In relation to the TSL shape a comparison analysis has been performed by considering a trapezoidal TSL for different hydrogen concentration values, as shown in **Figure 25**.

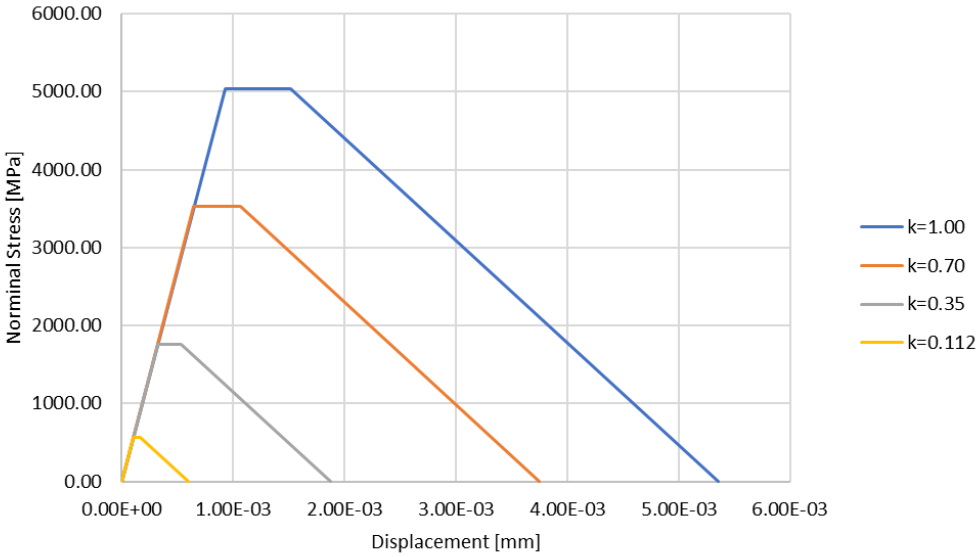

Figure 25. Trapezoidal TSL curves for different hydrogen concentration values.

As can be seen in **Figure 26**, for a specific SIF value of 41.2 $MPa\sqrt{m}$, the following analysis cases have been performed: Case A—Yellow (base case analysis), Case B—Green (numerical viscosity of 0.001) [35], Case C—Green (x-axis BCs applied at cohesive elements), Case D—Brown (Trapezoidal TSL as per **Figure 13**) and Case E—DarkBlue (Mixed discretisation scheme). All the analyses show similar crack propagation, which indicates the correct implementation of the numerical viscosity and BCs. The results also demonstrate the indepencce of the mechanical problem from the specific adopted TSL curve.

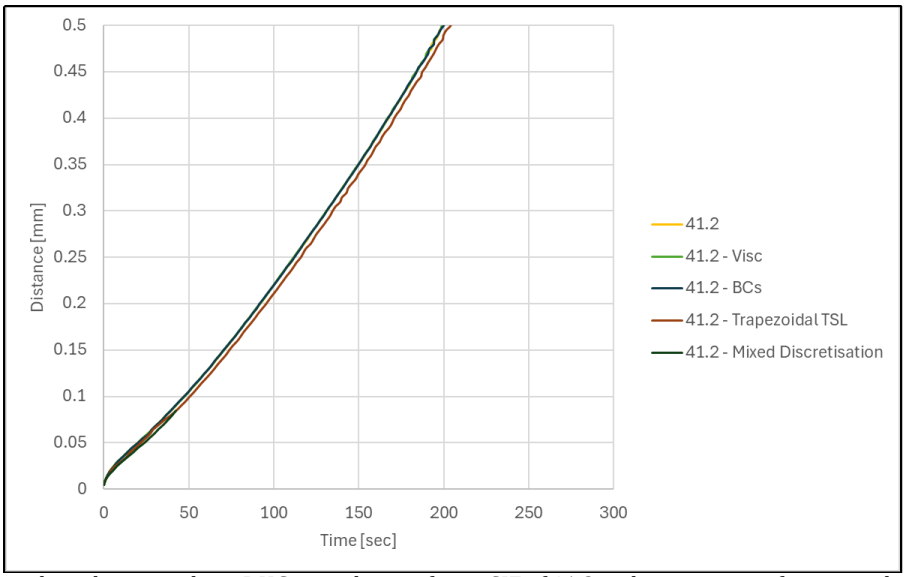

Figure 26. Crack length evolution without DHC contribution for an SIF of 41.2 and in presence of numerical viscosity parameter of 0.001, different BCs, considering the trapezoidal TSL, and mixed discretization schemes.

Additional sensitivity analysis has also been carried out to understand the influence of diffusivity parameters on the numerical analysis. **Figure 27** reports the results associated with an SIF value of 41.2 $MPa\sqrt{m}$, and three diffusivity parameters of 0.00253 mm^2/sec, 0.00250 mm^2/sec and 0.0026 mm^2/sec.

Figure 27. Crack length evolution without DHC contribution for an SIF of 41.2 and three difference hydrogen diffusivity parameters.

As expected, the crack propagation speed is directly proportional to the diffusivity parameter value, i.e., the cohesive elements degrade more rapidly due to higher velocity of hydrogen diffusion within the specimen.

4. Conclusions

In conclusion, hydrogen embrittlement (HE) is a critical degradation mechanism that severely impacts the structural integrity of high-strength metals, particularly in industries such as oil and gas, aerospace, and nuclear engineering. Finite element analysis (FEA) modelling has emerged as a powerful tool to predict HE-induced failures, enabling engineers to assess material behaviour under hydrogen exposure and optimize designs for enhanced safety and longevity. This study explores specific application cases of HE FEA modelling in engineering scenarios, with a focus on pipeline life prediction, while also discussing notable failure cases and future prospects to highlight the engineering value of this approach.

In pipeline engineering, HE FEA modelling plays a crucial role in predicting crack initiation and propagation under hydrogen-assisted stress corrosion cracking (H-SCC). For instance, high-pressure gas pipelines exposed to wet H_2S environments are prone to HE, leading to catastrophic failures if undetected. FEA models incorporating hydrogen diffusion, mechanical stress fields, and material damage criteria have been successfully applied to simulate crack growth rates and estimate remaining service life. A notable failure case is the 2000 gas pipeline rupture in New Mexico, attributed to H-SCC, which resulted in significant economic and environmental damage. Post-failure analyses validated by FEA demonstrated that hydrogen accumulation at stress concentrations accelerated crack propagation, underscoring the necessity of predictive modelling for risk mitigation.

Beyond pipelines, HE FEA has been applied in aerospace components, such as landing gear and turbine discs, where high-strength steels and titanium alloys are susceptible to hydrogen-induced delayed fractures. The 2018 failure of an aircraft component due to HE further emphasized the need for advanced simulation techniques to pre-emptively identify critical hydrogen thresholds.

The future prospects of HE FEA modelling are promising, particularly with advancements in multi-physics coupling (e.g., integrating electrochemical reactions with mechanical loading) and machine learning-assisted damage prediction. These developments will enhance predictive accuracy, enabling real-time structural health monitoring and optimized material selection. By reducing unplanned downtime and preventing failures, HE FEA modelling delivers substantial economic and safety benefits, reinforcing its indispensable role in modern engineering.

As discussed, this study presents an alternative approach to model absorbed hydrogen SCC in a sample test environment based on the HEDE predominant mechanism. The results confirm that the developed model can capture the fracture behaviour because of hydrogen embrittlement. The relationship and efficiency of the model application between laboratory specimens to real structural components is a critical aspect of structural engineering and materials science. The primary intent of the proposed numerical study is to replicate the tests performed in laboratory; however, since the results derived from the tests performed in laboratory (SENT and SENB testing activities) are largely used in the industry the final intent of the proposed numerical methodology is to provide a simplified and robust platform for understanding the performance of testing activities in presence of hydrogen.

In the proposed study and in accordance with the provided assumptions, the study has proven clear capability of the commercial software ABAQUS to predict crack propagation in presence of steel. It is important to note that the study does not introduce the steel material SMYS and/or SMTS as differentiated parameters, the numerical analysis has been performed considering material behaviour as linear elastic without introducing plasticity. The study also provides an alternative conservative approach to evaluate the crack propagation velocity in high-strength steel materials and results can be considered if the dynamic hydrogen coverage concept is implemented in the numerical analysis.

As is known from the literature that the presence

of hydrogen impacts the material behaviour since it changes the material comportment by reducing the plastic capability and providing a brittle failure mechanism (hydrogen embrittlement). This consideration is more evident in the presence of high-strength steel, where the elastic regime in absence of hydrogen is extended for high values of stress. In this case, the proposed model (omitting the plasticity components of the deformation) can be considered as a suitable numerical approximation where hydrogen neglects the possibility of the material being plastically deformed.

In conclusion, the study clearly highlighted the capability of capturing the correct physical problems and the crack velocity propagation implementing only standard elements (COH2D4T and CPE4T) within the software and without the need to develop external subroutines. The study tends also to highlight the criticality of implementing a correct TSL curve to simulate the dynamic hydrogen coverage within the specimen, the dependence of crack penetration velocity on the adopted TSL and also the independence from the specific TSL shape. Another important aspect/outcome highlighted by the study is the evident risk of underestimating the crack propagation speed if the dynamic hydrogen coverage is excluded in the analysis, which is a common approach used in the literature. For the analysis which include the dynamic hydrogen coverage, the numerical results tend to have a good approximation with the experimental data, however, some differences may be associated with variation in material properties, the role of the hydrogen trapping, the temperature of the specimen and the granular microstructure, which has not been considered in this study and can be considered in a future study. Developed framework can also be beneficial for other fracture modelling approaches such as extended finite element method (XFEM) [41–43] and peridynamics [44–48].

Author Contributions

Conceptualization, D.G., S.O. and E.O.; methodology, D.G. and S.O.; software, D.G.; validation, D.G.; formal analysis, D.G.; investigation, D.G., S.O. and E.O.; resources, D.G., S.O. and E.O.; data curation, D.G.; writing—original draft preparation, D.G.; writing—review and editing, S.O. and E.O.; visualization, D.G.; supervision, S.O. and E.O.; project administration, S.O.; funding acquisition, D.G. and S.O. All authors have read and agreed to the published version of the manuscript.

Funding

This work was funded by McDermott International.

Institutional Review Board Statement

Not applicable.

Informed Consent Statement

Not applicable.

Data Availability Statement

The data supporting these findings is available upon request.

Acknowledgments

The authors acknowledge McDermott International for the financial support.

Conflicts of Interest

The authors declare no conflict of interest.

References

[1] Veziroğlu, T.N., Sahin, S., 2008. 21st Century's energy: Hydrogen energy system. Energy Conversion and Management. 49, 1820–1831.

[2] Barreto, L., Makihira, A., Riahi, K., 2003. The hydrogen economy in the 21st century: A sustainable development Scenario. International Journal of Hydrogen Energy. 28, 267–284.

[3] Witkowski, A., Rusin, A., Majkut, M., et al., 2018. Analysis of compression and transport of the methane/hydrogen mixture in existing natural gas pipelines. International Journal of Pressure Vessels and Piping. 166, 24–34.

[4] Edwards, R.L., Font-Palma, C., Howe, J., 2021. The status of hydrogen technologies in the UK: A multi-

disciplinary review. Sustainable Energy Technologies and Assessments. 43, 100901. DOI: https://doi.org/10.1016/j.seta.2020.100901.

[5] The Oil & Gas Technology Centre, 2021. Phase 1 Project Report: Delivery of an offshore hydrogen supply programme via industrial trials at the Flotta Terminal – HOP Project HS413. Available from: https://assets.publishing.service.gov.uk/media/5e4ab9bf40f0b677ca249fed/Phase_1_-_OGTC_-_Hydrogen_Offshore_Production.pdf (cited 5 August 2025).

[6] Oil & Gas Authority, 2018. UKCS Decommissioning: 2018 Cost Estimate. Available from: https://www.nstauthority.co.uk/media/4925/decommissioning-cost-report-2018.pdf (cited 5 August 2025).

[7] De Meo, D., Diyaroglu, C., Zhu, N., et al., 2016. Modelling of stress-corrosion cracking by using peridynamics. International Journal of Hydrogen Energy. 41(15), 6593–6609.

[8] Lynch, S.P., 2011. Mechanistic and fractographic aspects of stress corrosion cracking (SCC). In: Raja V.S., Shoji T. (Eds.). Stress Corrosion Cracking - Theory and Practice. Woodhead Publishing Limited: Cambridge, UK.

[9] Wang, M., Akiyama, E., Tsuzaki, K., 2006. Determination of the critical hydrogen concentration for delayed fracture of high strength steel by constant load test and numerical calculation. Corrosion Science. 48, 2189–2202.

[10] Yatabe, H., Yamada, K., Rios de Los, E.R., et al., 1995. Formation of hydrogen-assisted intergranular cracks in high strength steels. Fatigue & Fracture of Engineering Materials & Structures. 18, 377–384.

[11] Miresmaeili, R., Ogino, M., Nakagawa, T., et al., 2010. A coupled elastoplastic-transient hydrogen diffusion analysis to simulate the onset of necking in tension by using the finite element method. International Journal of Hydrogen Energy. 35, 1506–1514.

[12] Djukic M.B., Zeravcic V.S., Bakic G.M., et al., 2014. Hydrogen embrittlement of low carbon structural steel. Procedia Materials Science. 3, 1167–1172.

[13] Troiano, A., 2016. The role of hydrogen and other interstitials in the mechanical behaviour of metals. Metallography Microstructure and Analysis. 5, 557–569. DOI: https://doi.org/10.1007/s13632-016-0319-4.

[14] Guzmán, A.A., Jeon, J., Hartmaier, A., et al., 2020. Hydrogen Embrittlement at Cleavage Planes and Grain Boundaries in Bcc Iron-Revisiting the First-Principles Cohesive Zone Model. Materials. 13, 5785. DOI: https://doi.org/10.3390/ma13245785.

[15] Robertson, I.M., Sofronis, P., Nagao, A., et al., 2015. Hydrogen embrittlement understood. Metallurgical and Materials Transactions B. 46, 1085–1103. DOI: https://doi.org/10.1007/s11663-015-0325-y.

[16] Zhao, Y.K., Seok, M.Y., Choi, I.C., et al., 2015. The role of hydrogen in hardening/softening steel: Influence of the charging process. Scripta Materialia. 107, 46–49.

[17] Liang, Y., Sofronis, P., Aravas, N., 2003. On the effect of hydrogen on plastic instabilities in metals. Acta Materialia. 51, 2717–2730.

[18] Stepanova, E., Grabovetskaya, G., Syrtanov, M., et al., 2020. Effect of Hydrogen on the Deformation Behavior and Localization of Plastic Deformation of the Ultrafine-Grained Zr–1Nb Alloy. Metals. 10, 592. DOI: https://doi.org/10.3390/met10050592.

[19] Djukic, M.B., Bakic, G.M., Sijacki Zeravcic, V., et al., 2016. Hydrogen embrittlement of industrial components: prediction, prevention, and models. Corrosion. 72 (7), 943–961.

[20] Djukic, M.B., Bakic, G.M., Sijacki Zeravcic, V.C., et al., 2016. Towards a unified and practical industrial model for prediction of hydrogen embrittlement and damage in steels. Procedia Structural Integrity. 2, 604–611.

[21] Sofronis, P., McMeeking, R.M., 1989. Numerical analysis of hydrogen transport near a blunting crack tip. Journal of the Mechanics and Physics of Solids. 37, 317–350.

[22] Krom, A.H.M., Bakker, A.D., 2000. Hydrogen trapping models in steel. Metallurgical and Materials Transactions B. 31, 1475–1482.

[23] Taha, A., Sofronis, P.A., 2001. A micromechanics approach to the study of hydrogen transport and embrittlement. Engineering Fracture Mechanics. 68, 803–837.

[24] Alvaro, A., Olden, V., Akselsen, O.M., 2013. 3D cohesive modelling of hydrogen embrittlement in the heat affected zone of an X70 pipeline steel. International Journal of Hydrogen Energy. 38, 7539–7549.

[25] Jiang, D.E., Carter, E.A., 2004. First principles assessment of ideal fracture energies of materials with mobile impurities: Implications for hydrogen embrittlement of metals. Acta Materialia. 52, 4801–4807.

[26] Serebrinsky, S., Carter, E.A., Ortiz, M., 2004. A quantum-mechanically informed continuum model of hydrogen embrittlement. Journal of the Mechanics and Physics of Solids. 52, 2403–2430.

[27] Sobhaniaragh, B., Afzalimir, S.H., Ruggieri, C., 2021. Towards the prediction of hydrogen–induced crack growth in high–graded strength steels. Thin-Walled Structures. 159, 107245. DOI: https://doi.org/10.1016/j.tws.2020.107245.

[28] Zhang, X., Lu, G., 2015. Multiscale Modelling of hydrogen embrittlement. Department of Physics and Astronomy, California State University Northridge: Northridge, CA, USA.

[29] Chen, Y.-S., Huang, C., Liu, P.-Y., 2024. Hydrogen trapping and embrittlement in metals — A review. International Journal of Hydrogen Energy. 136, 789–821. DOI: https://doi.org/10.1016/j.ijhydene.2024.04.076.

[30] Martínez-Pañeda, E., Golahmar, A., Niordson, C.F., 2020. A phase field formulation for hydrogen assisted cracking. Computer Methods in Applied Mechanics and Engineering. 342, 742–761. DOI: https://doi.org/10.1016/j.cma.2018.07.021.

[31] Wu, J.-Y., Mandal, T., Nguyen, V.P., 2020. A phase-field regularized cohesive zone model for hydrogen assisted cracking. Computer Methods in Applied Mechanics and Engineering. 358, 112614. DOI: https://doi.org/10.1016/j.cma.2019.112614.

[32] Yamde, A.A., Lade, V.G., Bindwal, A.B., 2024. Machine learning approaches for the prediction of hydrogen uptake in metal-organic-frameworks: A comprehensive review. International Journal of Hydrogen Energy. 98, 1131–1154. DOI: https://doi.org/10.1016/j.ijhydene.2024.12.131.

[33] Song, J., Curtin, W.A., 2012. Atomic mechanism and prediction of hydrogen embrittlement in iron. Nature Materials. 20(9), 1279–1284. DOI: https://doi.org/10.1038/nmat3479.

[34] Di Stefano, D., Mrovec, M., Elsässer, C., 2015. First-principles investigation of hydrogen trapping and diffusion at grain boundaries in nickel. Acta Materialia. 98, 306–312. DOI: https://doi.org/10.1016/j.actamat.2015.07.031.

[35] Muth, A., Fischer, C., Oeser, S., 2025. Fully coupled crystal plasticity and hydrogen diffusion modeling of X52 pipeline steel and weld microstructures. Computational Materials Science. 258, 114005. DOI: https://doi.org/10.1016/j.commatsci.2025.114005.

[36] Díaz, A., Alegre, J.M., Cuesta, I.I., 2016. A review on diffusion modelling in hydrogen related failures of metals. Engineering Failure Analysis. 66, 577–595.

[37] Oriani, R., 1970. The diffusion and trapping of hydrogen in steel. Acta Metallurgica. 18(1), 147–157.

[38] Hirose, Y., Mura, T., 1984. Growth mechanism of stress corrosion cracking in high strength steel. Engineering Fracture Mechanics. 19(6), 1057–1067.

[39] Hirose, Y., Mura, T., 1984. Nucleation mechanism of stress corrosion cracking from notches. Engineering Fracture Mechanics. 19(2), 317–329.

[40] Jadhav, D.N., Maiti, S.K., 2010. Characterization of stable crack growth through AISI 4340 steel using cohesive zone modelling and CTOD/CTOA criterion. Nuclear Engineering and Design. 240(4), 713–721. DOI: https://doi.org/10.1016/j.nucengdes.2009.11.042.

[41] Jha, A., Duhan, N., Singh, I.V., et al., 2025. Numerical study of the hydride embrittlement in zirconium alloy using XFEM. International Journal of Structural Stability and Dynamics. 25(2), 2440002. DOI: https://doi.org/10.1142/S0219455424400029.

[42] Kim, D.-H., Park, M.J., Chang, Y.S., et al., 2022. Evaluation of fracture properties of two metallic materials under hydrogen gas conditions by using XFEM. Metals. 12(11), 1813. DOI: https://doi.org/10.3390/met12111813.

[43] Kim, D.-H., Sim, J.M., Chang, Y.S., Baek, U.B., 2021. Hydrogen gaseous effects on fracture resistance of API-X70 estimated by XFEM. Journal of Mechanical Science and Technology. 35(9), 3829–3835. DOI: https://doi.org/10.1007/s12206-021-2106-7.

[44] Oterkus, E., 2022. Applications of Peridynamics in Marine Structures. Sustainable Marine Structures. 4(1), 13–15. DOI: https://doi.org/10.36956/sms.v4i1.475.

[45] Karpenko, O., Oterkus, S., Oterkus, E., 2022. Titanium Alloy Corrosion Fatigue Crack Growth Rates Prediction: Peridynamics Based Numerical Approach. International Journal of Fatigue. 162, 107023. DOI: https://doi.org/10.1016/j.ijfatigue.2022.107023.

[46] Chen, Z., Yang, D., Bian, H., 2023. Peridynamic Modeling of Crack Propagation Driven by Hydrogen Embrittlement. Engineering Fracture Mechanics. 293, 109687. DOI: https://doi.org/10.1016/j.engfracmech.2023.109687.

[47] Ran, X., Qian, S., Zhou, J., et al., 2022. Crack Propagation Analysis of Hydrogen Embrittlement Based on Peridynamics. International Journal of Hydrogen Energy. 47(14), 9045–9057. DOI: https://doi.org/10.1016/j.ijhydene.2021.11.173.

[48] Chen, Z., Yu, X., Yang, D., 2025. A Peridynamic Plastic Model for Hydrogen-Related Casing Pipe Damage of the Underground Hydrogen Storage. Computational Particle Mechanics. 1–26. DOI: https://doi.org/10.1007/s40571-025-00945-w.